

AD\_\_\_\_\_

Award Number: W81XWH-10-1-0518

TITLE: MASSIVELY PARALLEL ROGUE CELL DETECTION USING SERIAL TIME-  
ENCODED AMPLIFIED MICROSCOPY OF INERTIALLY ORDERED CELLS IN HIGH  
THROUGHPUT FLOW

PRINCIPAL INVESTIGATOR: BAHRAM JALALI

CONTRACTING ORGANIZATION: UNIVERSITY OF CALIFORNIA, LOS ANGELES  
Los Angeles, CA 90095-0001

REPORT DATE: August 2012

TYPE OF REPORT: Annual

PREPARED FOR: U.S. Army Medical Research and Materiel Command  
Fort Detrick, Maryland 21702-5012

DISTRIBUTION STATEMENT: Approved for Public Release;  
Distribution Unlimited

The views, opinions and/or findings contained in this report are those of the author(s) and should not be construed as an official Department of the Army position, policy or decision unless so designated by other documentation.

REPORT DOCUMENTATION PAGE				Form Approved OMB No. 0704-0188	
Public reporting burden for this collection of information is estimated to average 1 hour per response, including the time for reviewing instructions, searching existing data sources, gathering and maintaining the data needed, and completing and reviewing this collection of information. Send comments regarding this burden estimate or any other aspect of this collection of information, including suggestions for reducing this burden to Department of Defense, Washington Headquarters Services, Directorate for Information Operations and Reports (0704-0188), 1215 Jefferson Davis Highway, Suite 1204, Arlington, VA 22202-4302. Respondents should be aware that notwithstanding any other provision of law, no person shall be subject to any penalty for failing to comply with a collection of information if it does not display a currently valid OMB control number. <b>PLEASE DO NOT RETURN YOUR FORM TO THE ABOVE ADDRESS.</b>					
1. REPORT DATE August 2012		2. REPORT TYPE Annual		3. DATES COVERED 1 August 2011- 31 July 2012	
4. TITLE AND SUBTITLE Massively Parallel Rogue Cell Detection Using Serial Time-Encoded Amplified Microscopy of Inertially Ordered Cells in High Throughput Flow				5a. CONTRACT NUMBER	
				5b. GRANT NUMBER W81XWH-10-1-0518	
				5c. PROGRAM ELEMENT NUMBER	
6. AUTHOR(S) Bahram Jalali, Dino Di Carlo  E-Mail: jalali@ucla.edu				5d. PROJECT NUMBER	
				5e. TASK NUMBER	
				5f. WORK UNIT NUMBER	
7. PERFORMING ORGANIZATION NAME(S) AND ADDRESS(ES)  University of California, Los Angeles Los Angeles, CA 90095-0001				8. PERFORMING ORGANIZATION REPORT NUMBER	
9. SPONSORING / MONITORING AGENCY NAME(S) AND ADDRESS(ES) U.S. Army Medical Research and Materiel Command Fort Detrick, Maryland 21702-5012				10. SPONSOR/MONITOR'S ACRONYM(S)	
				11. SPONSOR/MONITOR'S REPORT NUMBER(S)	
12. DISTRIBUTION / AVAILABILITY STATEMENT Approved for Public Release; Distribution Unlimited					
13. SUPPLEMENTARY NOTES					
14. ABSTRACT- The aim of this project is to develop an instrument for high-throughput identification of rare circulating breast cancer cells to enable early detection and analysis of treatment effectiveness. While optical microscopy is useful for detailed examination of a small number of microscopic entities and hence identification of such cells, methods for conventional microscopy are incapable of statistically relevant evaluation and screening of large populations with high accuracy due to its low throughput and limited storage. During the second year of the CDMRP project, we succeeded in demonstrating an automated flow-through single-particle optical microscope that overcomes this limitation by performing sensitive blur-free image acquisition and non-stop real-time image-recording and classification of microparticles during high-speed flow. This is made possible by integrating ultrafast optical imaging technology, self-focusing microfluidic technology, optoelectronic communication technology, and information technology. To show the system's utility, we demonstrated high-throughput image-based screening of budding yeast and rare breast cancer cells in spiked blood with an unprecedented throughput of 100,000 particles/s and a record false positive rate of one in a million. Our results were published in Proceedings of the National Academy of Sciences in July 2012 ( <a href="http://www.pnas.org/content/early/2012/06/25/1204718109">http://www.pnas.org/content/early/2012/06/25/1204718109</a> ) and were also featured by UCLA Newsroom ( <a href="http://newsroom.ucla.edu/portal/ucla/world-s-fastest-camera-used-to-235979.aspx">http://newsroom.ucla.edu/portal/ucla/world-s-fastest-camera-used-to-235979.aspx</a> ).					
15. SUBJECT TERMS- breast cancer, flow cytometry, cell labeling, single cell imaging, automated microscope, flow through microscope, STEAM, time stretch					
16. SECURITY CLASSIFICATION OF:			17. LIMITATION OF ABSTRACT	18. NUMBER OF PAGES	19a. NAME OF RESPONSIBLE PERSON
a. REPORT	b. ABSTRACT	c. THIS PAGE			USAMRMC
U	U	U	UU	12	19b. TELEPHONE NUMBER (include area code)

## Table of Contents

	<u>Page</u>
Introduction.....	4
Body.....	6
Key Research Accomplishments.....	12
Reportable Outcomes.....	12
Conclusion.....	12
References.....	12

## Introduction

Optical microscopy is one of the most widely used methods in a diverse range of advanced research, industrial, and clinical settings including microelectronics, food science, oceanography, archaeology, environmental science, energy science, microbiology, mineralogy, and pathology. High information content spatial metrics provided by imaging are used to characterize microscopic particles such as emulsions, microorganisms, and cells in particle synthesis, ecosystem monitoring, biofuel formulation, drug discovery, histopathology, and cytology-based diagnostics. An impressive arsenal of optical nanoscopy methods enables imaging of cellular structures beyond the diffraction limit of light. Unfortunately, while there has been breathtaking progress in improving spatial resolution in the last two decades, mostly overlooked is the temporal resolution of imaging systems.

While useful for visual inspection of many individual microparticles without human intervention, conventional automated microscopy does not have high throughput and is hence unable to evaluate, analyze, and screen large populations with high statistical accuracy. High-throughput detection is essential to rapidly assay morphological and biochemical properties in a reasonable period of time. Unfortunately, the throughput of state-of-the-art automated microscopes is only up to  $\sim 1000$  particles/s, limiting the particle count. As a benchmark, this throughput is significantly lower than that of single-pixel high-throughput flow analyzers such as electronic particle counters and flow cytometers ( $\sim 100,000$  particles/s) which trade increased throughput for a lack of spatial resolution. Because of this trade-off, such systems are often unable to resolve single, multiple, and clustered particles or unusually shaped particles as well as to distinguish debris and nonspecific labeling and hence produce a large number of false positive events or inaccurate subpopulation counts.

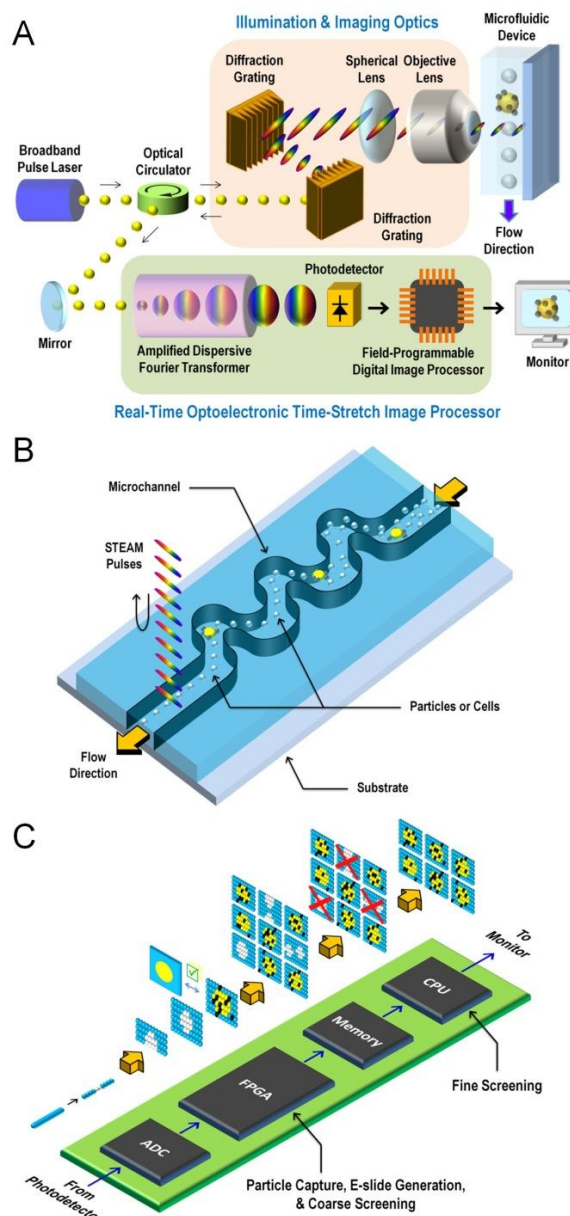


**Fig. 1. STEAM flow analyzer.** An animated video that shows the integrated functionality of the system is available. (A) Schematic of the STEAM flow analyzer that highlights the optical layout of the STEAM camera and real-time optoelectronic time-stretch image processor. The STEAM camera takes blur-free images of fast-flowing particles in the microfluidic device. The acquired images are optoelectronically processed and screened in the real-time optoelectronic time-stretch image processor. (B) Microfluidic device in which particles are controlled to flow at a uniform velocity and focused and ordered by inertial lift forces in the microfluidic channel. (C) Field-programmable digital image processor that captures particles and performs fully automated particle classification in real time. It consists of (i) a high-speed analog-to-digital converter (ADC), (ii) a field-programmable gate array (FPGA) for particle capture, E-slide generation, and coarse particle classification, (iii) an on-board memory circuit for storing selected E-slides, and (iv) a central processing unit (CPU) for fine particle classification.

While high-end digital cameras [i.e., charge-coupled device (CCD) and complementary metal-oxide-semiconductor (CMOS) cameras] are now able to perform imaging at a speed approaching 1 million frames/s, they are not well suited for high-throughput microscopy. First, a critical limitation that hampers imaging of particles flowing at high speeds is the relatively long shutter speed or exposure time ( $\geq 1$  microsecond) that results in motion blur and loss of resolution during the high-speed flow, hence degrading specificity. Another limitation is the time needed to download the image from the array of thousands of pixels. To achieve high frame rates, the number of pixels that are employed must be reduced in a process known as partial readout. The penalty is that image resolution is lost at high frame rates. Furthermore, there is a fundamental trade-off between sensitivity and speed – at high frame rates, fewer photons are captured during each frame, leading to reduction in sensitivity. Finally, currently digital image processing cannot be performed in real time due to the storage and access of the massive amount of digital data that is produced during high-speed imaging and hence requires many days of off-line digital processing. This translates into a limited particle count, thus compromising statistical accuracy in high-throughput screening. These limitations prevent automated microscopy from analyzing a large population of particles with high statistical accuracy in a practical period of time.

To address the needs and fill in the technological gap between the automated microscope and high-throughput flow analyzer, we propose and demonstrate an automated flow-through single-particle optical microscopy system that can evaluate, analyze, and screen a large population of particles with high specificity, high sensitivity, and high statistical accuracy in a short time. This method builds on an unique integration of (i) an ultrafast optical imaging modality known as serial time-encoded amplified microscopy (STEAM) for blur-free imaging of particles in high-speed flow, (ii) inertial microfluidic technology for sheath-free focusing and ordering of particles with inertial forces, and (iii) hybrid optoelectronic image processing circuitry for real-time image processing. The integrated system transforms particles in well-controlled microfluidic flow into a series of E-slides – an electronic version of glass slides – on which particles of interest are digitally analyzed. With the power of optoelectronic communication and information technologies, this property enables fully automated real-time image-recording and classification of a large number of particles through their morphological and

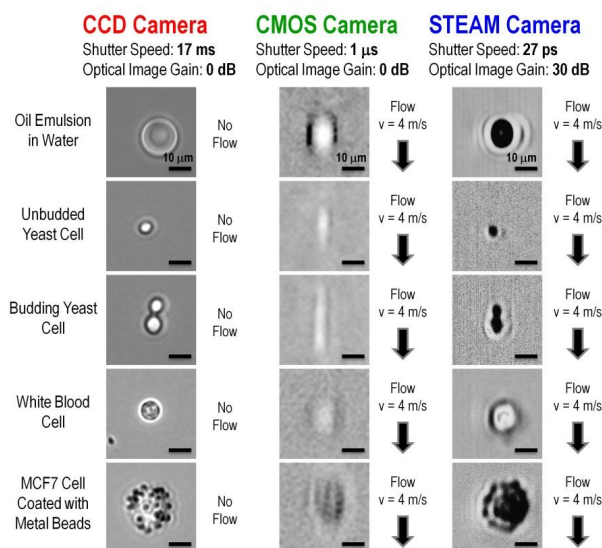


**Fig. 2. Performance of the STEAM camera and comparison with a conventional CCD camera and a state-of-the-art CMOS camera.** E-slides of flowing particles of various species in the microfluidic device were generated by the STEAM flow analyzer with the built-in STEAM camera (27 ps shutter speed, 128 x 512 pixels, 25 dB optical image gain). The E-slides are compared with images of the same particles captured by a state-of-the-art CMOS camera (1 microsecond shutter speed, 32 x 32 pixels, no optical image gain) under the same flow. To operate at these high speeds, the CMOS camera used partial readout, limiting the number of pixels to 32 x 32. Here the particles were controlled to flow at a uniform speed of 4 m/s, which corresponds to a throughput of 100,000 particles/s based on the volumetric flow rate. The high-speed motion of the particles was frozen by the ultrafast shutter speed (ultrashort exposure time) of the STEAM camera (27 ps) yet without sacrificing sensitivity due to the optical image amplification whereas the reduced sensitivity and motion blurs caused by the CMOS camera's much lower shutter speed and lack of optical image amplification are evident. For further comparison, stationary particles of the same types on a glass slide were obtained under a conventional microscope with a CCD camera with a much longer exposure time (17 ms shutter speed, 1280 x 1024 pixels, no optical image gain). Despite the fact that the STEAM camera is many orders of magnitude faster than the CCD camera, the two cameras share similar image quality (i.e., sensitivity and resolution).

biochemical features. To demonstrate our technology's utility, we show real-time non-stop image-based identification and screening of budding yeast cells at different budding stages and rare breast cancer cells in blood with an unprecedented throughput of 100,000 particles/s and a record false positive rate of one in a million.

## Results

Principle of the high-throughput imaging flow analyzer. Our system, which we refer to as the STEAM flow analyzer (Fig. 1A), consists of three subsystems: (i) the microfluidic device (Fig. 1B), (ii) the STEAM camera (Fig. 1A), and (iii) the real-time optoelectronic time-stretch image processor (Fig. 1C). An animated video shows the integrated functionality of the system. The STEAM flow analyzer operates in three steps. First, particles are controlled to flow at a uniform velocity and focused and ordered by inertial lift forces in the microfluidic channel. Second, the STEAM camera takes images of the fast-flowing particles. Finally, the real-time optoelectronic time-stretch image processor processes the images optically and electronically and then performs automated particle screening in real time.

The STEAM flow analyzer employs inertial microfluidic technology (Fig. 1B). This method provides uniform positions and velocities for particles through intrinsic inertial lift forces (important for generation of clear E-slides) while eliminating the need for sheath fluid which is traditionally required for hydrodynamic focusing in conventional flow cytometers. While inertial forces are typically assumed to be negligible in microfluidic systems, they can, in fact, be important when the flow rate in microchannels is high. Particles in finite-inertia confined channel flows focus to cross-sectional dynamic equilibrium positions that correspond with the fold of symmetry of the channel cross section. Furthermore, longitudinal ordering (i.e., stabilized interparticle or intercell spacing along the length of the channel) results from inertial lift forces and the flow field acting together. In some of our previous work, we determined an optimal balance between inertial lift forces and Dean drag forces, counter-rotating vortices perpendicular to primary channel flow, to accurately position a range of particle sizes to a single streak with two heights within the channel at a high flow rate. Here we reduced the length of one of these optimized channels to decrease its pressure and lowered the height of the channel to bring the distinct equilibrium positions in the vertical plane into closer proximity. To ensure stability in real-time image processing, the microfluidic device was fabricated by replica molding in thermoset polyester due to its high stiffness and ability to sustain high pressures.

The STEAM camera first captures fast sequential images with laser pulses and then stretches image-encoded pulses in time so that they can be digitized and processed in real time (See Materials and Methods). During the time-stretch process, images are also optically amplified to overcome the thermal noise inherent in photon-to-electron conversion. In the first step, a pair of diffraction gratings spatially disperses the broadband optical pulse into a rainbow designed to capture 1D line scans of particles flowing through the channel. The temporal duration of these pulses is 27 ps (shutter speed) and they occur at a repetition rate of 36.7 MHz (line scan rate). The back-reflected pulses from the microfluidic device are directed via an optical circulator toward the real-time optoelectronic time-stretch image processor followed by the high-speed photodetector and the field-programmable digital image processor. 2D E-slides are then constructed from the digitized 1D frames and made available for screening.

As shown in Fig. 1A, the real-time optoelectronic time-stretch image processor consists of an amplified dispersive Fourier transformer, a high-speed photodetector, and a field-programmable digital image processor. First, the amplified dispersive Fourier transformer serializes the image-encoded pulse (i.e., the 1D image frame) into a pixel stream that is slowed down in time so that it can be digitized and processed in real time. While it is being stretched in time, the image-carrying pulse is amplified in the optical domain through distributed Raman amplification in the time-stretch element. Raman amplification is chosen as it has a broad and flexible optical spectrum and also leads to low noise figure in the frequency-to-time mapping process. The optical image amplification ( $\sim 1000\times$ ) before photon-to-electron conversion is critical as it enables high-throughput microscopy in the ultrashort exposure time (27 ps) without the need for a high-intensity illuminator. In addition, the ultrafast shutter speed freezes any motion of particles in high-speed flow, allowing for acquisition of blur-free images. The amplified 1D data stream is detected by the high-speed single-pixel photodetector, eliminating the need for a detector array and hence readout time limitations. After analog-to-digital conversion by a real-time digitizer, the data is processed in real time in the field-programmable digital image processor with a programmable multi-stage decision-making architecture (Fig. 1C) that employs a field-programmable gate array (FPGA), an on-board memory circuit, and a central processing unit (CPU). Specifically, the function of the FPGA is to identify the presence of particles (ignoring the unimportant

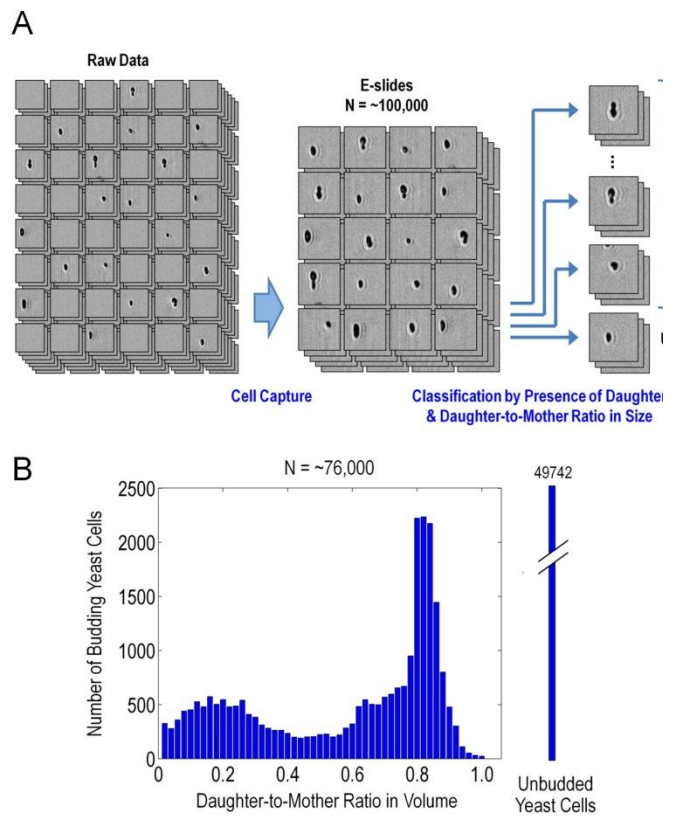


**Fig. 3. High-throughput screening of budding yeast with the STEAM flow analyzer.** (A) Screening process of the field-programmable digital image processor. The FPGA performs cell capture while ignoring the blank images between cells and stores the corresponding E-slides into the on-board memory. The CPU then distinguishes between budding and unbudded cells, classifies the budding cells by daughter-to-mother ratio in size, and finally generates a histogram for the subpopulations. (B) Subpopulation analysis of yeast at different stages of budding. The total number of captured yeast cells is 75509, about 34% of which constitutes budding cells. Here the entire procedure that consists of the measurement, image analysis, and histogram generation takes less than a few minutes. Since the STEAM flow analyzer operates in real time, time-resolved statistical analysis of the subpopulations can also be performed to control and optimize the budding process. Furthermore, similar capture and subpopulation analysis can also be applied to emulsions for applications in cosmetics and pharmaceuticals.

space between the particles), generate E-slides for the particles, coarsely down-select the slides (i.e., the particles) through their morphological and biochemical markers, and store those selected in the memory. As a second-step screening process, the CPU performs fine particle classification on the stored slides with more stringent algorithms such as decision-tree classification and supervised learning methods.

The STEAM flow analyzer's blur-free image acquisition enables differentiation of particles from a heterogeneous population. Fig. 2 shows E-slides of fast-flowing particles of various species in the microfluidic channel captured by the STEAM flow analyzer. Here the particles were controlled to flow at a uniform speed of 4 m/s, which corresponds to a throughput of 100,000 particles/s – a very fast flow, but motion blur is absent in the images due to the ultrafast shutter speed of the STEAM camera (27 ps). For comparison, Fig. 2 also shows images of the same types of particles under the same flow conditions captured by a state-of-the-art CMOS camera. These images show that the CMOS camera's lower shutter speed (1 microsecond) and lack of optical image amplification significantly reduced the sensitivity and caused motion blur in the images, rendering the camera unable to classify particles reliably. For further comparison, stationary particles of the same types on a glass slide were obtained under a conventional microscope with a CCD camera with a much longer exposure time (shutter speed) of 17 ms (Fig. 2). Despite the fact that the STEAM camera is many orders of magnitude faster than the CCD camera, the two cameras share similar image quality (i.e., sensitivity and resolution).

Screening of budding yeast with the high-throughput imaging flow analyzer. To show the utility of the STEAM flow analyzer, we used it to demonstrate high-throughput screening of *Saccharomyces cerevisiae*, commonly known as budding yeast. Budding yeast are important in food science, are used as a model for studying eukaryotic cell biology, and are engineered to produce protein therapeutics. Growth in yeast can be studied and optimized by flow cytometry or microscopy – both of which possess specific limitations. Biochemical analysis alone via flow cytometry is insufficient for analysis of complex checkpoints and detection of minor perturbations in the cell cycle and provides poor characterization of the asymmetric growth of yeast in comparison with imaging. A high-throughput microscopy technique such as our STEAM flow analyzer could provide a powerful screening tool to assay morphological changes potentially accompanying systematic gene knockouts or other molecular perturbations.



The STEAM flow analyzer can efficiently identify and screen budding yeast cells and perform subpopulation analysis in real time. Here we programmed the FPGA and CPU to capture incoming cells, distinguish between budding and unbudded cells, and classify budding cells based on different budding stage (Fig. 3A). Specifically, the FPGA performs cell capture while ignoring the blank images and stores the corresponding E-slides in the on-board memory (1 GB)

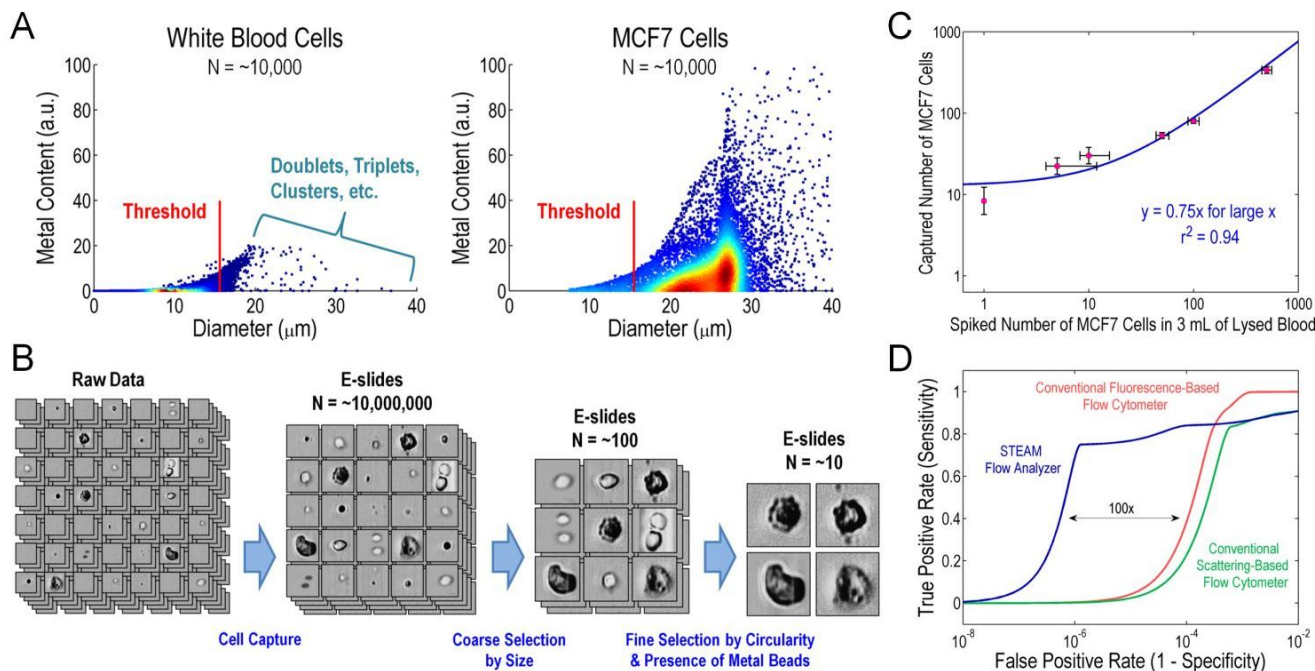


**Fig. 4. Rare cell detection with the STEAM flow analyzer.** (A) Scatter plots of white blood cells and MCF7 cells based on the cell size (i.e., area) and the presence of the surface antigens (i.e., metal beads). The total number of events is  $\sim 10,000$  for both cell types. This statistical analysis is used to build a model and train the supervised learning method and hence the algorithms to run the field-programmable digital image processor. The threshold for the size-based selection performed on the FPGA is set such that smaller MCF7 cells are also selected at the expense of detecting larger white blood cells. The rare white blood cell events that overlap with the distribution of MCF7 cells are doublets or clusters and can hence be rejected by imaging (which is not possible with single-point detection methods). (B) Selection process of the field-programmable digital image processor. The FPGA performs cell capture, coarse size-based classification, and filters out more than 99.9995% of white blood cells while leaving only  $\sim 100$  false positive events per mL of lysed blood along with true positive events. The CPU then performs fine classification by circularity and presence of metal beads and further down-selects cells by an order of magnitude, leaving true positive events and  $\sim 10$  false positive events per mL of lysed blood which arise due to image processing artifacts which can further be rejected by human visual inspection. (C) Statistical analysis of the system's capture efficiency for various concentrations. The results indicate that the field-programmable digital image processor can identify extremely rare cells with a high efficiency of 75% (limited by the imperfect coating efficiency and missing smaller MCF7 cells in the FPGA selection process). Here all the measurements were performed with bead-coated MCF7 cells spiked in buffer containing white blood cells from 3 mL of lysed blood ( $\sim 80$  million white blood cells) at a throughput of 100,000 cells/s. Individual samples were measured four times, establishing that the classification is highly repeatable (indicated by the vertical error bars). Moreover, the correlation of detected MCF7 cells with spiked MCF7 cells is good ( $r^2 = 0.94$ ). The horizontal deviations can be attributed to several known sources of error in the spiking method including the initial hemacytometer count. (D) ROC curve analysis of the STEAM flow analyzer in comparison with the conventional flow cytometer. Our method is sufficiently sensitive for detection of  $\sim 1$  MCF7 cell in a million white blood cells (i.e., a false positive rate of  $\sim 10^{-6}$ ) and is two orders of magnitude better in terms of false positive rate than the conventional flow cytometer yet without sacrificing throughput.

which can save up to  $\sim 16,000v$  slides (each of which has  $64/v$  KB), where  $v$  is the flow speed in units of m/s. Here since the 2D E-slides are constructed from a series of 1D frames with the second dimension provided by the flow, the size of each slide decreases and hence the total number of slides that can be saved in the memory increases as the flow speed increases. We estimate that the flow speed can be set up to 8 m/s (corresponding to 200,000 cells/s) while retaining reasonable image quality and classification accuracy. The saved E-slides are then subject to the CPU's classification process in which the budding yeast cells are isolated and classified by daughter-to-mother ratio in size to

generate a histogram for the subpopulations using a decision-tree classification method (Fig. 3B). For comparison, we also performed normal microscopic observation of yeast cells with a CCD camera and performed digital image processing similar to the automated classification on the CPU in the STEAM flow analyzer and found good agreement between our high-throughput method and the conventional method, suggesting that the STEAM flow analyzer is useful for analysis of yeast growth behavior with high statistical accuracy. Since the STEAM flow analyzer operates in real time, time-resolved statistical analysis of the subpopulations can also be performed to control and optimize the budding process. Furthermore, similar capture and subpopulation analysis with real-time feedback is expected to be useful for optimization of emulsions for applications in cosmetics and pharmaceuticals.

**Rare cell detection with the high-throughput imaging flow analyzer.** To further show the utility of the STEAM flow analyzer, we used it to demonstrate rare cell detection. While statistically insignificant and hence often ignored, rare events among a large heterogeneous population of cells in blood such as hematopoietic stem cells, antigen-specific T cells, and circulating tumor cells are important in biomedical research as well as medical diagnostics and therapeutics. Such rare cells can be identified by a combination of morphological (i.e., size, circularity, and clustering) and biochemical (i.e., surface antigens) markers. Here our model for rare cells is the MCF7 cell line (breast cancer) spiked in blood. Red blood cells are lysed with a hypotonic lysing agent while MCF7 cells are fixed with formaldehyde and coated with metal beads with a diameter of 1 micron via an antibody to EpCAM (a cell surface molecule that exists on the surface of epithelial cells, but not on the surface of blood cells). Our observation under a conventional microscope indicates that ~80% of MCF7 cells are coated with 5 – 20 metal beads.

To demonstrate how surface marker detection could be achieved and coupled with morphological analysis in our system, we performed off-line statistical analysis of white blood cells and coated MCF7 cells. This validation is important as it is required to build a fully trained model for our supervised learning method or support vector machine (SVM) to be implemented on the FPGA and CPU. The SVM model predicts whether a new target (i.e., cell) falls into any of the pre-defined cell categories and is then used to identify the target cells in real time. Fig. 4A shows scatter plots of white blood cells and MCF7 cells based on the cell size (i.e., diameter) and presence of surface antigens (i.e., metal beads) produced by our system. The plots indicate that the system is capable of differentiating most white blood cells and MCF7 cells with high specificity using a single molecular marker.

With the fully trained cell classification model, the STEAM flow analyzer can detect MCF7 cells as rare as ~1 in a million in a short period of time. Here we programmed the FPGA and CPU such that the FPGA captures incoming cells and performs size-based cell classification while the CPU performs classification by circularity and presence of metal beads. The threshold for the size-based selection is set such that smaller MCF7 cells are also selected at the expense of detecting larger white blood cells (Fig. 4A). Yet, this process efficiently rejects more than 99.9995% of white blood cells, all residual red blood cells, and all free-floating metal beads, leaving only a small number of false positive events (~100 per mL of lysed blood) along with true positive events (Fig. 4B). The FPGA's ability to filter out the large

number of blood cells and avoid storing the massive amount of digital data enables non-stop real-time operation. The down-selected E-slides (i.e., cell images) are stored in the memory (1GB) which can save up to  $\sim 4000v$  slides (each of which has  $256/v$  KB), where  $v$  is the flow speed in units of m/s as described above. The stored slides are then subject to the CPU's selection process in which the cells are further classified by circularity and presence of metal beads. This process rejects almost all the false positive events (i.e., multiple, unfocused, or unordered white blood cells) that have survived from the initial selection process on the FPGA while leaving true positive events and a very small number of false positive events ( $\sim 10$  per mL of lysed blood) which arise due to image processing artifacts and can further be rejected by human visual inspection.

Our statistical analysis of the capture efficiency indicates that the field-programmable digital image processor can identify extremely rare cells with a high efficiency of 75% (limited by the imperfect coating efficiency and missing smaller MCF7 cells in the FPGA selection process) (Fig. 4C). Furthermore, our receiver operating characteristic (ROC) curve analysis of the results indicates that our method is sufficiently sensitive for detection of  $\sim 1$  MCF7 cell in a million white blood cells and is 100 times better in terms of false positive rate than the conventional flow cytometer (Fig. 4D), yet without sacrificing throughput. Here all the measurements were performed at a throughput of 100,000 cells/s, corresponding to screening of 10 mL of lysed blood in less than 15 minutes.

## Discussion

We have developed a high-throughput single-microparticle flow-through image analyzer for real-time image acquisition and screening of a large heterogeneous population of particles. By overcoming the technological limitations that exist in conventional automated microscopes (with many pixels and  $\sim 1,000$  particles/s throughput) and high-throughput flow analyzers (with a single pixel and  $\sim 100,000$  particles/s throughput), our system has achieved real-time image-based screening with high sensitivity ( $\sim 75\%$ ), high specificity (one in a million), and high statistical accuracy ( $\sim 100,000$  particles/s) simultaneously. Here the throughput is only limited by the microfluidic device's tolerance to high pressures caused by high flow rates, not the STEAM camera's image acquisition speed or the field-programmable digital image processor's processing speed. We estimate that the throughput can be increased to 200,000 particles/s while retaining reasonable image quality and classification accuracy. Our method can also be combined with a conventional cell sorter to sort out rare target cells for further genetic analysis of the cells. Furthermore, our method can, in principle, work at shorter wavelengths for higher spatial resolution, provided that proper optical components are available.

While in our proof-of-concept demonstration, we showed high-throughput screening of budding yeast and detection of rare breast cancer cells spiked in blood, our method should also be amenable to other applications in which high-throughput microscopy is required. Such applications include imaging and detection of bioparticles of interest in oceanography (e.g., phytoplanktons), energy science (e.g., oil emulsions and engineered microbes), environmental science, food science, cosmetics, pharmaceuticals, and medicine.

## Key Research Accomplishments

1. Integration of optics, microfluidics, digital and analog electronics, and algorithms to realize a ultrahigh throughput automated flow-through microscope
2. Detection of rare MCF7 breast cancer cells in lysed blood with a sensitivity of one in a million – a record value and one that represents 100x improvement over the current state-of-the-art Fluorescence Activated Cell Sorter (FACS).

## Reportable Outcomes

Realization of an automated high-throughput flow-through microscope with the ability to detect one MCF7 breast cancer in a million white blood cells

1. B. Jalali, K. Goda, and K. K. Tsia, “Apparatus and method for optically amplified imaging,” US 2010/0141829 A1 (2010)
2. B. Jalali, K. Goda, and K. K. Tsia, “Apparatus and method for dispersive Fourier-transform imaging,” US 12/985539 (2010)
3. K. Goda et al, “High-throughput single-microparticle imaging flow analyzer,” *PNAS* doi:10.1073/pnas.1204718109 (2012)

## Conclusion

In summary, we have developed a high-throughput single-cell flow-through image analyzer for real-time image acquisition and screening of a large heterogeneous population of cells with high sensitivity and high statistical accuracy. The throughput is limited by the microfluidic device’s tolerance to high pressures caused by high flow rates, not the STEAM camera’s image acquisition speed as well as the field-programmable digital image processor’s processing speed. We estimate that the throughput can be increased to 200,000 cells/s while classification accuracy. Our method can also be combined with a conventional cell sorter to sort out rare cells for further chemical analysis of the cells. While in our proof-of-concept demonstration, we showed high-throughput screening of budding yeast and detection of rare breast cancer cells in blood, our method should also be amenable to other applications in which high-throughput microscopy is required, such as those found in oceanography, energy science, and medicine.

## References

- [1] K. Goda et al., “Serial time-encoded amplified imaging for real-time observation of fast dynamic phenomena,” *Nature* 458, 1145 (2009)
- [2] K. Goda et al, “High-throughput single-microparticle imaging flow analyzer,” *PNAS* doi:10.1073/pnas.1204718109 (2012)